AIAA Aviation
13-17 June 2016, Washington, D.C.
34th AIAA Applied Aerodynamics Conference

Model Reduction in Discrete-Vortex Methods for 2D Unsteady Aerodynamic Flows

ArunVishnu SureshBabu[1]*, Kiran Ramesh[2],†
and Ashok Gopalarathnam[1]‡
[1]*Department of Mechanical and Aerospace Engineering, North Carolina State University, Raleigh, NC 27695-7910*
[2]*Department of Aerospace Sciences, School of Engineering, University of Glasgow, United Kingdom*

In this paper, we propose a method for model reduction in discrete-vortex methods. Discrete vortex methods have been successfully employed to model separated and unsteady airfoil flows. Earlier research revealed that a parameter called the Leading Edge Suction Parameter (LESP) can be used to model leading-edge vortex (LEV) shedding in unsteady flows. The LESP is a measure of suction developed at the leading edge, and whenever the LESP exceeds a critical value, a discrete vortex is released from the leading edge so as to keep the LESP at the critical value. Although the method was successful in predicting the forces on and the flow field around an airfoil in unsteady vortex-dominated flows, it was necessary to track a large number of discrete vortices in order to obtain the solution. The current study focuses on obtaining a model with a reduced number of discrete vortices to model LEVs, thus improving the computation time. Vortex shedding from the leading edge is modeled by a shear layer that comprises a few discrete vortices, and a single concentrated vortex whose strength varies with time. The single vortex at the end of the shear layer accounts for the concentrated vortical structure that comprises several discrete vortex elements in conventional vortex methods. A merging algorithm is initiated when the edge of the shear layer starts rolling up. Suitable discrete vortices are identified using a kinematic criterion, and are merged to the growing vortex at every time step. The reduced order method is seen to bring down the number of discrete vortices required to model LEV structures significantly.

Nomenclature

α	pitch angle, angle of airfoil chord with inertial horizontal
$\dot{\alpha}$	pitch rate
$\dot{h}$	plunge rate
$\eta(x)$	variation of camber along airfoil
$\gamma(x,t)$	chordwise vorticity distribution
Γ_b	bound circulation of airfoil t
Γ_{lev_n}	strength of n^{th} leading edge vortex
Γ_{tev_m}	strength of m^{th} trailing edge vortex
ϕ_B	velocity potential from bound circulation
ϕ_{lev}	velocity potential from leading edge vortices
ϕ_{tev}	velocity potential from trailing edge vortices

*Graduate Research Assistant, asuresh2@ncsu.edu
†Lecturer in Aerospace Engineering, Kiran.Ramesh@glasgow.ac.uk, +44 1413307392, Member, AIAA
‡Professor, Box 7910, agopalar@ncsu.edu, (919) 515-5669, Associate Fellow, AIAA
The latest version of this paper is available at http://www.mae.ncsu.edu/apa/publications.html

θ	variable of transformation of chordwise distance
a	pivot location on the airfoil from 0 to 1 (x/c)
$A_0, A_1, A_2....$	Fourier coefficients
$Bxyz$	body frame
c	airfoil chord
C_d	drag coefficient
C_l	lift coefficient
C_m	pitching moment coefficient
h	plunge displacement
K	non dimensional pitch rate
$LESP$	Leading Edge Suction Parameter
$Oxyz$	inertial frame
t	time
t^*	nondimensional time = $\frac{tU}{c}$
U	freestream velocity
$W(x,t)$	local downwash
x	chordwise distance
DV	Discrete Vortex
LDVM	LESP modulated Discrete Vortex Method
LESP	leading edge suction parameter
LEV	Leading Edge Vortex
TEV	Trailing Edge Vortex

I. Introduction

Unsteady aerodynamic phenomena are prevalent in a large number of problems in modern aerospace engineering research. These include dynamic stall in wind turbines and helicopter rotors, and flapping-wing vehicle (micro-air vehicle) design. These problems are characterised by apparent-mass effects, flow separation and leading-edge vortex (LEV) formation and shedding. Unsteady flows with intermittent LEV formation are the focus of the current research. The LEV influences the flowfield tremendously, and is responsible for an enhancement in lift while it is present above the wing and also large nose-down pitching moments and flow separation over the entire airfoil when it convects either off the trailing edge or away from the airfoil.[1,2]

Methods of simulating the physics and effects of unsteady aerodynamic phenomena date back to Wagner[3] and Theodorsen.[4] The application of these theoretical methods is however limited by their assumptions such as attached flow, small amplitude motion and planar wake structure. For unsteady flows with vortex shedding such as those considered in the present study, experiments and high-fidelity computations have facilitated fundamental studies of the underlying phenomena. McGowan et al.,[5] Ol et al.,[6] Garmann & Visbal[7] and Granlund et al.[8] have analysed the forces and flowfields for such unsteady motions over a broad parameter space using both experimental and computational methods. Pitt Ford & Babinsky,[9] Baik et al.[10] and Rival et al.[11] have studied leading edge vortices using experimental techniques. These methods are not suitable for the initial phases of aerodynamic/control design because of cost and time considerations. This has been the motivation of many researchers to construct low-order models for unsteady simulation of wings and airfoils.

Discrete-vortex methods have been successfully used in past decades to model unsteady separated flows. These methods are usually based on potential-flow theory, and the shear layers depicting separated flow are shed from the surface in the form of discrete vortices. Clements & Maull[12] and Saffman & Baker[13] have written detailed reviews on the historical development of the discrete-vortex method. A review on more recent applications of vortex methods for flow simulation is given by Leonard.[14] Sarpkaya,[15] Clements,[16] Kiya & Arie,[17] amongst other researchers, have applied this category of methods successfully to model flow past inclined plates and bluff bodies. Katz[18] has developed a discrete-vortex method for separated flow past an airfoil, where the location of separation on the airfoil has to be prescribed using information from experiments or other means. More recently, low-order methods based on discrete vortices have been developed by Ansari et al.,[19] Wang & Eldredge,[20] Ramesh et al.[21] to model leading edge vortices in unsteady flows, with applications toward insect flight and MAV aerodynamics. Though these methods are based on

potential theory, they capture the essential physics in flows of interest by combining inviscid theory with discrete-vortex shedding. Apart from providing a means to calculate the force coefficients on the airfoil, these methods also enable the study of flow features. These are significant advantages of this class of methods over semi-empirical methods, which only allow determination of the force coefficients through empirical fitting.

Many of the methods cited above assume some *ad-hoc* start and stop criteria for discrete-vortex shedding, such as continuous shedding from a given location (valid only for sharp edges) or shedding that starts and stops depending on whether the local angle of attack exceeds a critical value (valid only for a small range of motions). A more general vortex shedding criterion is required to make discrete-vortex methods broadly applicable to a wide range of geometries (including airfoils with rounded leading edges) and arbitrary unsteady motions. Ramesh et al.[21] have developed a discrete-vortex aerodynamic method to model unsteady flows with intermittent LEV shedding using a leading-edge suction parameter (LESP). The unique aspect of this method (LESP-modulated discrete vortex method, or, LDVM) is that vortex shedding is turned on or off at the leading edge using a criticality condition. This method is, therefore, ideally suited to modeling oscillatory airfoil flows in which intermittent LEV shedding is a key feature. In comparison with semi-empirical methods in which several parameters are typically used, for a given airfoil and a given Reynolds number, this model uses only a single empirical constant, the critical LESP, and is a highly physics-based approach.

LDVM has been shown to be successful in predicting forces and moments on the airfoil, as well as flow field around the airfoil for high-frequency unsteady maneuvers. However, it is necessary to track a significant number of discrete vortices in order to obtain the instantaneous forces and moments on the airfoil. The computational complexity increases as $\mathcal{O}(n^2)$ (when fast summation methods are not used), where n is the number of vortices in the flowfield, resulting in possibly large computing times. The computational time of any discrete vortex model can be significantly decreased by reducing the number of discrete vortices. The current study focuses on obtaining a model with a reduced number of leading edge vortices, thus improving the computation time.

The popular Brown-Michael model[22] was one of the earliest efforts towards modeling the leading edge vorticity using reduced number of vortices. Specifically, the Brown-Michael model used a single vortex with time-varying strength to represent the vorticity shed from a delta wing. Wang and Eldredge[23] recently improved on this model to derive analytic expressions for the evolution of single vortices using impulse matching for a flat plate. Howe[24] has presented a generalized correction for the Brown-Michael model, and uses the model to study the effect of the translating vortex of time-varying strength on a rigid half-plane. One vortex with time-varying strength models the leading edge vorticity, while another similar vortex is used to represent the trailing edge vorticity. Cortelezzi and Leonard[25] used a single vortex with time-dependent strength to model the shear-layer roll up of a semi-infinite plate. This model was further revised to accommodate a shear layer feeding vorticity into a growing vortex.[26] Some of these models use an unsteady Kutta condition at the leading edge to find the strength of the single vortex that models the LEV.

Several experimental studies have been conducted by various researchers to understand the evolution of the leading-edge-vortex structure. The shear layer emanating from the leading edge starts rolling up into a concentrated vortex. Vorticity is fed into this concentrated vortex structure by the shear layer, and it grows in strength. In case of prolonged vorticity shedding, the leading edge vortex pinches off from the shear layer, and is convected downstream. Meanwhile, a new vortex roll-up is initiated near the leading edge.[27,28,29] Antonini et al.[30] use semi-empirical data to model the expanse of the time-varying vortex core.

Several articles can be found in the literature that address the merging of discrete vortices to reduce the count of discrete vortices in the flow field.[31,32,33] For example, Nair and Taira[34] give a network theoretic approach to identify important vortex-vortex interactions, and obtain a sparsified model that accurately predicts the dynamics of the original system based on these interactions. The conditions used for merging are based on closeness, relative velocity etc. between vortex pairs. The criterion to identify rollup in the model presented in the current work is based on angular velocity between vortex pairs at the tip of the shear layer. Additionally, a discrete vortex is merged with the growing vortex based on its closeness, relative and angular velocities with respect to the growing LEV.

The current research aims to model LEV structures using a reduced-order model, by representing an LEV as a single concentrated vortex structure, connected to the leading-edge through a shear layer. The shear layer is modeled by a certain number of discrete vortices shed from the leading edge. A kinematic condition is used to to predict the initial rollup of the shear layer. Once the rollup is identified, a merging

algorithm based on another kinematic condition is implemented to merge discrete vortices from the shear layer to the concentrated vortex at the tip of the shear layer at every time step. This approach replicates a shear layer that feeds vorticity into a leading-edge vortex of increasing strength.

Necessary theoretical background is briefly described in the next section. A description of the reduced order model, and the merging algorithm then follows this in Section III. Finally, we compare the results of the reduced-order model and LDVM.

II. Background

1. *Large-angle unsteady thin-airfoil theory*

A large-angle unsteady thin-airfoil theory is used in this method to model the flow around a 2D body undergoing unsteady motion that may involve translation and rotation in the plane of motion. It is based on the time-stepping approach of Katz and Plotkin.[35] The reference frames used for the mathematical formulation are shown in Figure 1. $Oxyz$ represents the inertial frame, and the body frame, $Bxyz$, is a frame that is attached to the body in motion. The two frames coincide at time $t = 0$. For $t > 0$, the body frame moves towards the left. Trailing edge vorticity is shed at every time step in the form of discrete vortex so as to satisfy the Kutta condition.

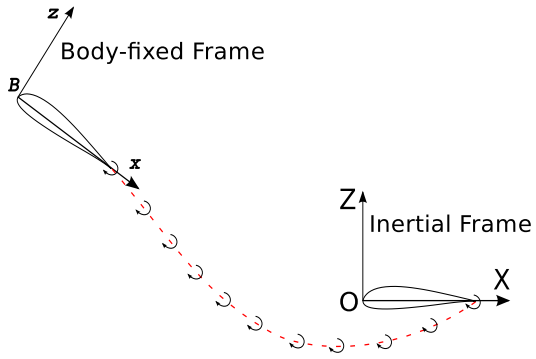

Figure 1. An illustration of the time-stepping method.

Following the lines of thin airfoil theory, the airfoil in motion is replaced by a vorticity distribution along its chord length $\gamma(x)$, which is represented by a Fourier series.

$$\gamma(\theta, t) = 2U \left[A_0(t) \frac{1 + \cos\theta}{\sin\theta} + \sum_{n=1}^{\infty} A_n(t) \sin(n\theta) \right] \tag{1}$$

where θ can be related to the chordwise coordinate x through a transformation,

$$x = \frac{c}{2}(1 - \cos\theta) \tag{2}$$

Here, U is the magnitude of the airfoil's translational velocity along the X axis. $A_0(t)$, $A_1(t)$, ..., $A_n(t)$ are the Fourier coefficients at time t. The Fourier series representation of the vorticity distribution implicitly enforces the Kutta condition which requires the vorticity to be zero at the trailing-edge. The Fourier coefficients at a time step can be obtained by enforcing the zero normal flow boundary condition at the airfoil surface.

$$A_0(t) = -\frac{1}{\pi} \int_0^{\pi} \frac{W(x,t)}{U} d\theta \tag{3}$$

$$A_n(t) = \frac{2}{\pi} \int_0^{\pi} \frac{W(x,t)}{U} \cos n\theta d\theta \tag{4}$$

Equations 3 and 4 give the Fourier coefficients as a function of the induced velocity normal to the airfoil surface, $W(x,t)$, henceforth referred to as downwash. The downwash is the result of induced velocities from the discrete vortices in the flow field and due to the motion kinematics. The plunge velocity in the Z direction, $\dot{h}$, the pitch angle of the chord, α, and its rate of change, $\dot{\alpha}$, are parameters that influence the downwash due to the motion of the body. These are shown in Figure 2. The downwash can be written as:

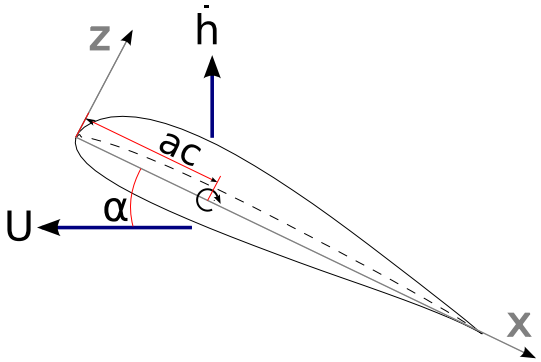

Figure 2. Airfoil velocities (positive as shown) and pivot location.

$$W(x,t) \equiv \frac{\partial \phi_B}{\partial z} = \frac{\partial \eta}{\partial x}(U\cos\alpha + \dot{h}\sin\alpha + \frac{\partial \phi_{lev}}{\partial x} + \frac{\partial \phi_{tev}}{\partial x}) - U\sin\alpha - \dot{\alpha}(x-ac) + \dot{h}\cos\alpha - \frac{\partial \phi_{tev}}{\partial z} - \frac{\partial \phi_{lev}}{\partial z} \quad (5)$$

where ϕ_B is the velocity potential of the bound vorticity distribution, and ϕ_{lev} and ϕ_{tev} are the velocity potentials associated with the discrete leading edge and trailing edge vortices. $\eta(x)$ represnts the camber distribution of the airfoil. The strength of a trailing edge vortex shed at a time step is determined iteratively so as to enforce Kelvin's circulation condition, which is given by:

$$\Gamma_b(t) + \sum_{m=1}^{N_{tev}} \Gamma_{tev_m} + \sum_{n=1}^{N_{lev}} \Gamma_{lev_n} = 0 \quad (6)$$

$\Gamma_b(t)$ is the bound circulation obtained as the integral of bound vorticity over the chord:

$$\Gamma_b(t) = Uc\pi \left[A_0(t) + \frac{A_1(t)}{2} \right] \quad (7)$$

2. *LESP criterion for initiation of LEV formation LEV shedding and termination criteria*

It has been shown by Ramesh et. al[36] that the initiation and termination of leading-edge vorticity shedding is determined by a nondimensional measure of the suction at the leading edge. It has also been shown that this leading edge section parameter (LESP) is the same as leading coefficient A_0 in the Fourier series representing the bound vorticity. Thus,

$$LESP(t) = A_0(t) \quad (8)$$

A given airfoil has a critical value of LESP for a given Reynolds number. This value is independent of motion kinematic parameters such as amplitude, reduced frequency, and pivot location. Once the critical value of LESP of a given airfoil is obtained for a given Reynolds number using data from experiment or CFD for a sample motion, LDVM can predict the initiation and termination of intermittent leading-edge vorticity in any arbitrary motion of the airfoil at that Reynolds number.

The instant at which the magnitude of LESP exceeds the critical value marks the initiation of leading edge vorticity shedding. A discrete leading edge vortex (LEV) is shed at every time step after initiation

of leading edge vorticity shedding. the strength of the vortex at a time step is determined so as to keep the LESP at its critical value. If the LESP is positive, the sign of the discrete vortex shed at the leading edge is clockwise, and the discrete vortex tends to get convected towards the upper surface. On the other hand, when the LESP is negative,the sign of the discrete vortex is counter clockwise, and it gets convected towards the lower surface. Vorticity shedding terminates when the magnitude of LESP comes below the critical value.

We follow the vortex placement method followed by Ansari et al.[37] to determine the position of the discrete vortex (DV) generated at either edge at any instant of time. It is placed at one third of the distance between the shedding edge and the previously shed vortex. The first DV shed when LEV formation starts is placed using the velocity at the leading edge. Like other discrete vortex methods, the point vortices are convected with the flow velocity at the location of the vortices. A first-order time stepping process is used since the change in accuracy was not much when high-order methods were used. Using a vortex model with core radius v_{core}, we have from Vatistas et al.[38] that the induced velocities (u and w) by the k^{th} vortex in the X and Z direction are:

$$u = \frac{\gamma_k}{2\pi} \frac{Z - Z_k}{\sqrt{((X - X_k)^2 + (Z - Z_k)^2)^2 + v_{core}^4}} \tag{9}$$

$$w = -\frac{\gamma_k}{2\pi} \frac{X - X_k}{\sqrt{((X - X_k)^2 + (Z - Z_k)^2)^2 + v_{core}^4}} \tag{10}$$

Details of force and moment calculations in the discrete vortex method can be found in Ramesh et al.[36]

III. The reduced order model

This reduced order model is developed to phenomenologically model the evolution of leading vortex structures as revealed by experimental and high fidelity CFD studies. In the early stages of leading-edge vorticity shedding, a shear layer is ejected from the leading edge. The tip of this shear layer rolls up into a core after some time. Once the roll-up is initiated, the shear layer keeps feeding vorticity into the core until either the vorticity shedding stops, or the core pinches off from the shear layer.

LDVM predicts this flow pattern using discrete vortices shed from the leading edge for the period of time during which the LESP exceeds the critical value.The objective of the reduced order model is to reduce the discrete vortex count in LDVM by merging suitable pairs of discrete vortices shed from the leading edge. In particular, the large number of discrete vortices that represent a huge concentrated vortex core can be replaced by one single vortex that has the combined strength of all the discrete vortices.

We are interested in studying the growth of the core through a model that incorporates a shear layer, and a concentrated vortex at its tip. There are two steps in modeling this phenomenon. The first is the identification of the rollup of the shear layer. Once the shear layer starts rolling up, a vortex that grows in strength with time is introduced at the tip of the shear layer. At each time step, some vorticity is added to this growing single LEV (referred to as SLEV henceforth) by merging an appropriate DV to it. This procedure results in a few point vortices forming a shear layer, from which vorticity is fed into the growing SLEV.

A. Initial rollup

It is proposed that the shear layer starts rolling up when there is a relative rotation between any two successive vortices near the tip of the shear layer. For identifying the onset of rollup, we keep track of the angular velocity of successive vortex pairs in a shear layer. When the angular velocity $\omega_{i,i-1}$ between the i^{th} and $(i-1)^{th}$ vortices in the shear layer exceeds a threshold value, the shear layer is assumed to have started rolling up at its tip. The i^{th} LEV is declared as the SLEV.

B. Merging algortihm

As observed by researchers like Moore,[33] Sarpkaya[32] and Cortelezzi,[31] when two like vortices come near each other, they start rotating about the centroid. If one is significantly stronger than the other, the weaker one

appears to be revolving about the stronger one since the centroid would nearly coincide with the location of the stronger vortex. In either case, the separation between the vortices keeps decreasing, and tends to a steady state value in the absence of influence from any other external agents or boundaries. Essentially, they behave as a system that can be approximated by a single vortex at the centroid, with a strength that is equal to the combined strength of the two vortices. Following these observations, and deriving insight from the flow pattern predicted by LDVM, we propose a merging algorithm that uses the angular velocity of the line joining the SLEV and a discrete vortex in the LEV, the component of relative velocity along this line and the separation between them as the metrics for determining if the discrete LEV has to be merged with the SLEV.

The relative velocity of two vortices along the line joining can be obtained in terms of the relative distance vector $\bar{R}_{21}$ connecting their positions, and their relative velocity $\bar{V}_{21}$ as,

$$\bar{V}_{rel} = \bar{V}_{21}.\bar{R}_{21} \tag{11}$$

The angular velocity, Ω_{21} between two point vortices can be expressed as,

$$\Omega_{21} = \frac{\bar{V}_{21}.\bar{R}^{\perp}_{21}}{|\bar{R}^{\perp}_{21}|} \tag{12}$$

where $\bar{R}^{\perp}_{21}$ is the vector normal to $\bar{R}_{21}$.

At every time step after rollup is identified, the algorithm finds a DV within a specified distance $|\bar{R}_{21}|$ from the SLEV that has the maximum angular velocity Ω about the SLEV or the maximum approach speed $\bar{V}_{rel}$ towards the SLEV. This DV is merged to the SLEV, and the combined discrete vortex is convected with the velocity induced at its new location.

The search is necessary in the initial phase of rollup when there can be a quite a few discrete vortices that start rotating about the SLEV. At this stage, the shear layer may even start rolling up very close to the leading edge. However, it has been observed that, within a few time steps after rollup is initiated, the straight shear layer and the concentrated vortex structure become clearly distinguishable. At this stage, the search for a suitable merge candidate is not necessary anymore. Vorticity can be fed into the SLEV by merging the DV at the tip of the shear layer.

We have used a model with a common vortex-core radius for all the discrete vortices, to prevent the induced velocities from becoming unbounded when two point vortices come close to each other.[36] The distance used for searching in the merging algorithm has been set by trial and error to a value that is 10 times this core radius. The threshold angular velocity to identify initial rollup was set to 0.001 rad/s. Also, it was observed that the search in the merging algorithm could be stopped after 10 discrete vortices were merged to the SLEV.

After this, the DV at the tip of the shear layer is merged to the SLEV at every time step. The number of DVs in the shear layer is approximated by the relation:

$$n_{shear} = \frac{distance\ of\ SLEV\ from\ LE}{0.75 * core\ radius\ of\ the\ DVs} \tag{13}$$

If the number of DV's in the shear layer is greater than this value at any time step, the DV at the tip of the shear layer is merged to the SLEV. This replicates the shear layer feeding vorticity into the vortex core.

C. Location of the combined DV

When two DVs of strengths Γ_1 and Γ_2 located at X_1 and X_2 respectively are merged, it has been customary to add their strengths and place the combined vortex at the centroid of the two DVs given by:

$$X_{centroid} = \frac{\Gamma_1 X_1 + \Gamma_2 X_2}{\Gamma_1 + \Gamma_2} \tag{14}$$

However, this approach induces errors in the flow field especially if the merging takes place near the airfoil.[31] Cortelezzi (1992) proposed a merging scheme in which the combined vortex is placed at a different location from the centroid so as to conserve the velocity at the shedding location. Following this idea, we propose a novel merging scheme in which the merged DV is placed at a location referred to as the optimal location,

(x_{opt}, z_{opt}). By placing the combined vortex at this location, we ensure that the Fourier coefficients A_0 and A_1 are conserved before and after merging. This conserves the leading-edge suction, as well as the bound circulation of the airfoil given by

$$\Gamma_b = \pi c U \left[A_0 + \frac{A_1}{2} \right] \tag{15}$$

A 2D Newton iteration is employed to determine (x_{opt}, z_{opt}) that conserves A_0 and A_1.

D. Identifying pinch-off

In some cases, the shear layer stops feeding vorticity into the LEV when it attains a maximum strength. This is followed by the LEV getting convected downstream, and the shear layer starting to rollup near the LE to form a new LE vortex structure. We refer to this as LEV 'pinch-off'. To model this phenomenon, we monitor the DVs in the shear layer at every time step. If, at any time step, two adjacent DVs in the shear layer have opposite signs for their angular velocities with respect to the SLEV, a pinch-off is declared to be identified. Following this, the DV in this vortex pair that is close to the LE is declared as a new SLEV. The search algorithm is again initiated to find matching DVs to merge with this SLEV. Meanwhile, the DVs at the edge of the shear layer associated with the first SLEV are merged to it, one at every time step. Thus, the first SLEV represents the LEV structure that pinches off from the shear layer, and the new SLEV models the vortex core that starts rolling up near the LE.

E. Intermittent LEV shedding

A new LEV is shed each time the LESP reaches the critical value. This is referred to as intermittent LEV shedding. The reduced order model handles this by initiating a new SLEV whenever LESP reaches its critical value. Each SLEV and its shear layer capture the concentrated core and the shear layer structure associated with the individual LEVs.

IV. Results

In this section, we present a comparison of the results of the reduced order model with those of the LDVM for three cases.

A. Case 1: Flat plate undergoing 0-90 pitching motion about LE

In Case 1, we study a flat plate that is pitching about its leading edge at a Reynolds number of 1,000. The smoothed ramp motion is generated using Eldredge's canonical formulation.[23] At the end of the motion, the pitch angle reaches a value of 90 degrees. A non dimensional pitch rate value of $K = 0.2$ is used for this motion. The critical value of LESP for a flat plate at a Re of 1,000 is 0.11.[36] Fig. 3 shows the comparison of LESP variation predicted by the two methods, along with the coefficients of lift, drag and moment. A comparison of the streamline patterns predicted by the two methods at five different instants of time are shown in 4.

In this case, the LESP reaches its positive critical value in LDVM during the pitch-up phase of motion, as can be seen from Fig. 3. This marks the onset of leading-edge vortex shedding from the upper surface of the plate. The LESP remains at the critical value till the end of the motion. This results in an uninterrupted shedding of leading edge vorticity during the remaining span of motion. The evolution of this LEV structure in the LDVM can be observed in the streamline plots in Fig. 4. The DVs representing the LEV are also marked in these plots using red dots. The shear layer ejected from the leading edge soon rolls up into a concentrated vortical structure on the upper surface near the leading edge. This structure continues to grow in size as the shear layer keeps rolling up and feeding vorticity into it. A thin shear layer that connects the concentrated core to the leading edge is apparent soon after the shedding starts. This shear layer elongates when the concentrated vortex core convects away from the plate. The concentrated LEV core is attached to the LE through this thin shear layer until the end of the motion.

The reduced order model exactly predicts the onset of LEV shedding and thereafter closely replicates the flow field. This can be seen from the streamline patterns of the reduced order method in Fig. 4. An SLEV

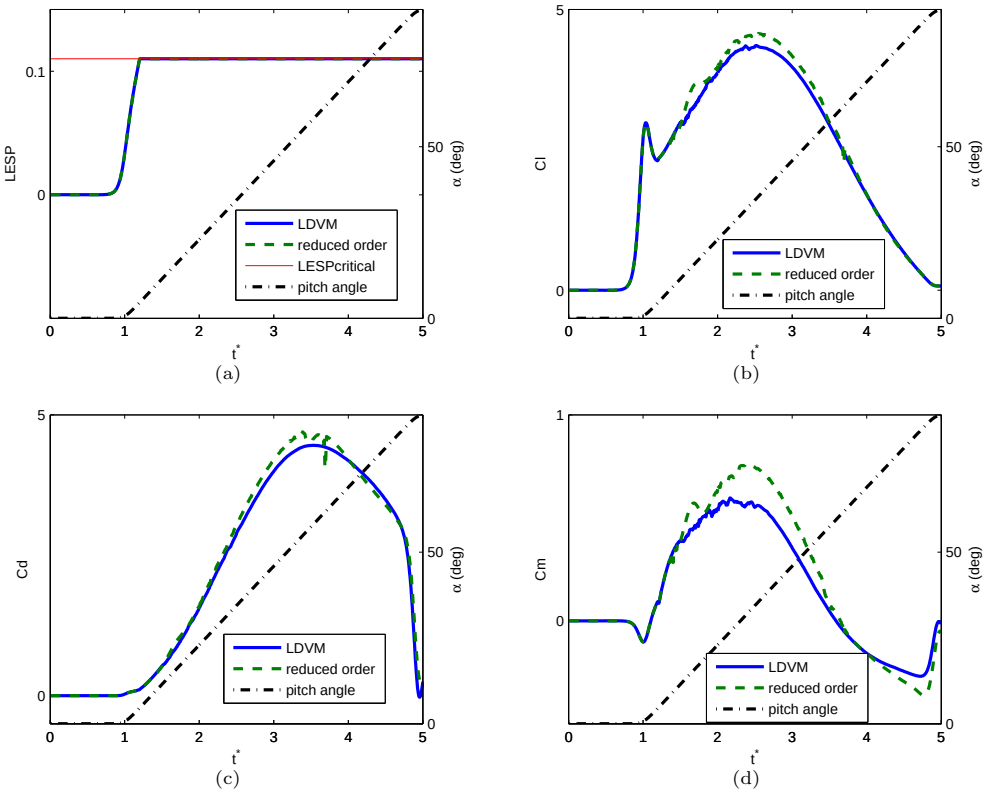

Figure 3. Case 1: Comparison of predictions of the reduced order method and LDVM. Variation with $t^* = tU/c$ of: (a) LESP, (b) lift coefficient, (c) drag coefficient, and (d) pitching moment coefficient about the mid chord.

is initiated as soon as the relative rotation between a pair of DVs at the tip of the shear layer exceeds the threshold value. Following this, one DV is merged to the SLEV at every time step using the search criterion. After 10 DVs are merged to the SLEV, the search is terminated, and the merging is done based on the approximate shear layer length given by (13). By this time, the thin shear layer and the concentrated core structure of the LEV is apparent in LDVM ($t^* = 1.3$). During the later time steps, the SLEV in the reduced order model represents the strength and position of concentrated vortex core of LDVM. The elongated shear layer connects the SLEV to the leading edge.

The comparison of the results show that lift and drag coefficient histories as well as the history of coefficient of moment about the mid-chord predicted by the reduced order model agree well with those predicted by LDVM. At the last time step, there are 380 DVs in LDVM that accounts for the vorticity shed from the leading edge during the period of time for which LESP was above its critical value. Meanwhile, the reduced order model can predict this flow field by using just 89 DVs. Corresponding to the decrease in the number of discrete LEVs in the flowfield, the run time for the reduced order (20.1 s) is smaller compared to that of LDVM (29.3 s).

B. Case 2: SD7003 airfoil undergoing 0-90-0 pitching motion about trailing edge

In this study, we consider an SD7003 airfoil undergoing a pitch up-return motion. It undergoes a smoothed 0-90-0 pitch up-return motion with the pivot point at the trailing edge. A non dimensional pitch rate of $K = 0.4$ is used for this motion. The critical value of LESP for an SD7003 airfoil at a Reynolds number of 100,000 is 0.14. The comparison of LESP and the time variations of force and moment coefficients between the two methods are shown in Fig. 5. Figure 6 presents a comparison of the streamline patterns predicted by the two methods at different instants of time.

The LESP value for this motion reaches the critical value during the pitch-up phase, as shown in Fig. 5.

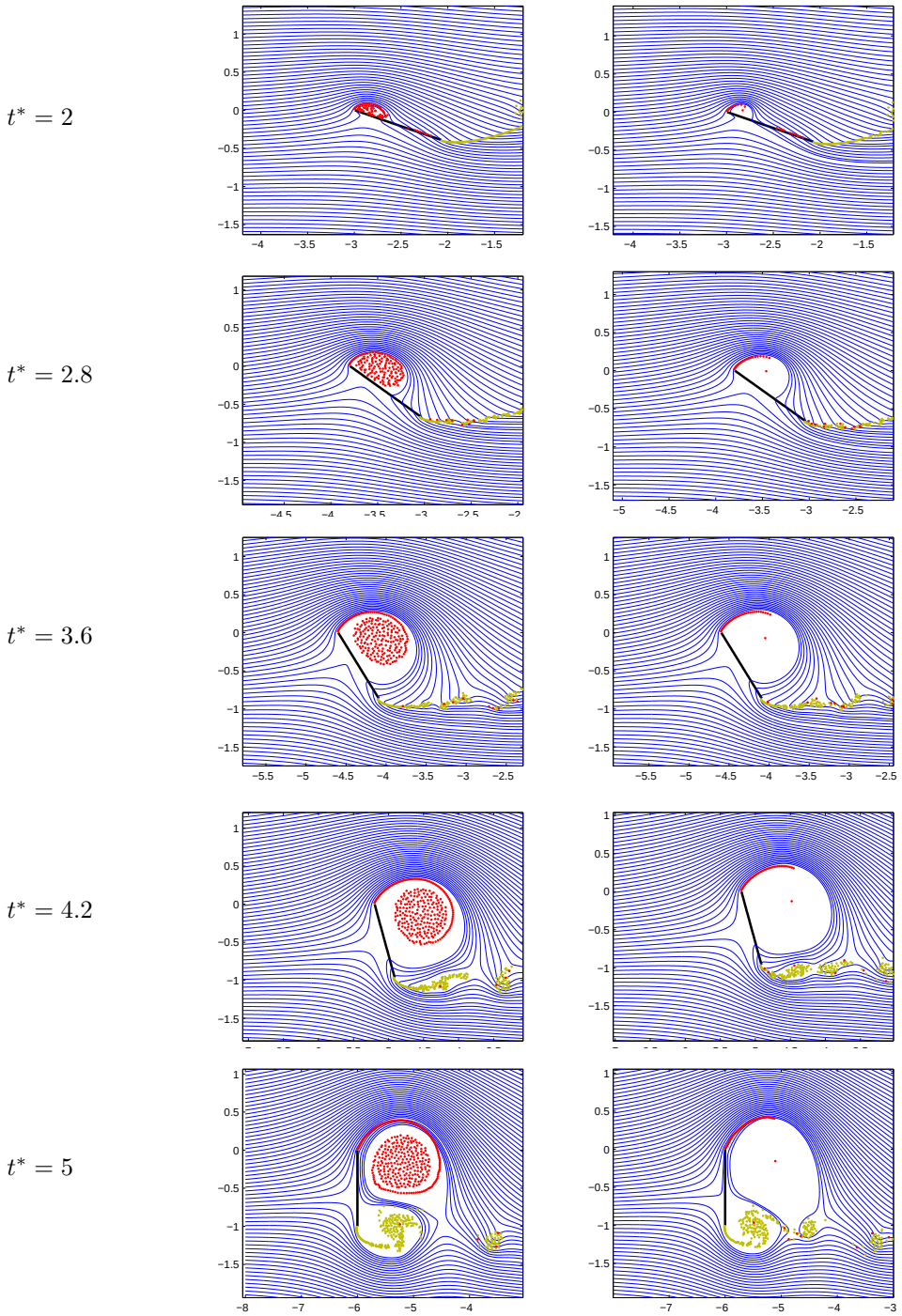

Figure 4. Case 1: Streamline patterns predicted by LDVM (left) and the reduced order method (right) at five time instants.

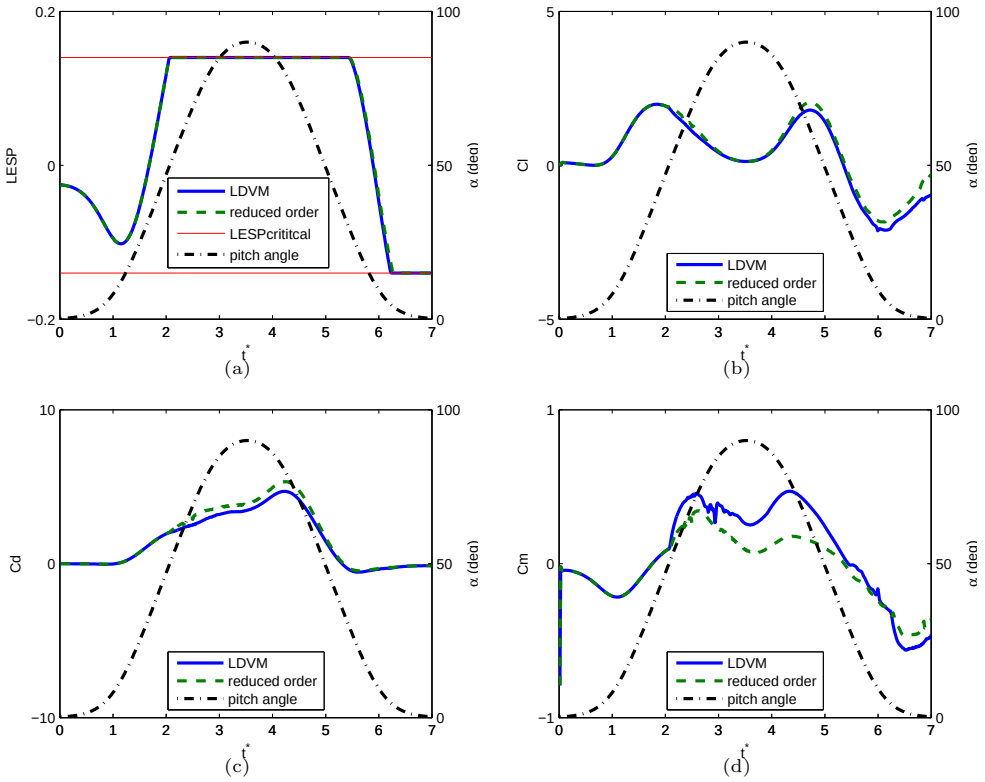

Figure 5. Case 2: Comparison of predictions of the reduced order method and LDVM. Variation with $t^* = tU/c$ of: (a) LESP, (b) lift coefficient, (c) drag coefficient, and (d) pitching moment coefficient about the quarter chord.

It remains at the critical value for some time, and comes down during the return phase. This indicates that vorticity is shed from the leading edge from the middle of the pitch-up phase to the middle of the return phase. The LESP value reaches the negative critical value towards the end of the motion, indicating the shedding of another LEV from the lower surface. Thus, this is a case where intermittent LEV shedding occurs. Fig. 6 shows the evolution of the flow field predicted by LDVM for this case. The shear layer associated with the first LEV starts rolling up near the LE. This vortex continues to grow until the vorticity shedding stops. When the shedding terminates, the shear layer detaches from the leading edge. The vortex structure and the shear layer get convected downstream, and they interact with the trailing edge vorticity. Meanwhile, vorticity shedding starts again at the leading edge on lower surface after a short pause. This shear layer can be seen to be rolling up near the leading edge towards the end of the motion.

Comparison of LESP histories of the two methods show that the reduced order model predicts the onset and termination of leading edge vorticity shedding at the same instants of time as LDVM. The reduced order model captures the above mentioned features of the flowfield as can be seen from the streamline plots in Fig. 6. It predicts the roll-up of the first shear layer successfully, and models the subsequent growth of the leading edge vortex very closely to the predictions of LDVM using an SLEV. The SLEV remains attached to the leading edge through a shear layer of varying length airfoil until the vortex shedding stops. During this period of time, the shear layer is seen to add vorticity to the SLEV. Upon the termination of vorticity shedding, the shear layer detaches from the leading edge, and the DVs in the shear layer continue to be merged with the SLEV in the following time steps. When the LESP reaches the critical value for the second time, a new SLEV is initiated to capture the new LEV structure. Meanwhile, the DVs in the shear layer associated with the first SLEV are being merged with the first SLEV.

The force coefficient histories of the two methods are in good agreement, except for the slight discrepancy towards the end of the motion when the interaction between LEV and trailing edge vorticity takes place. The coefficient of moment about the quarter chord predicted by the reduced order method, however, shows

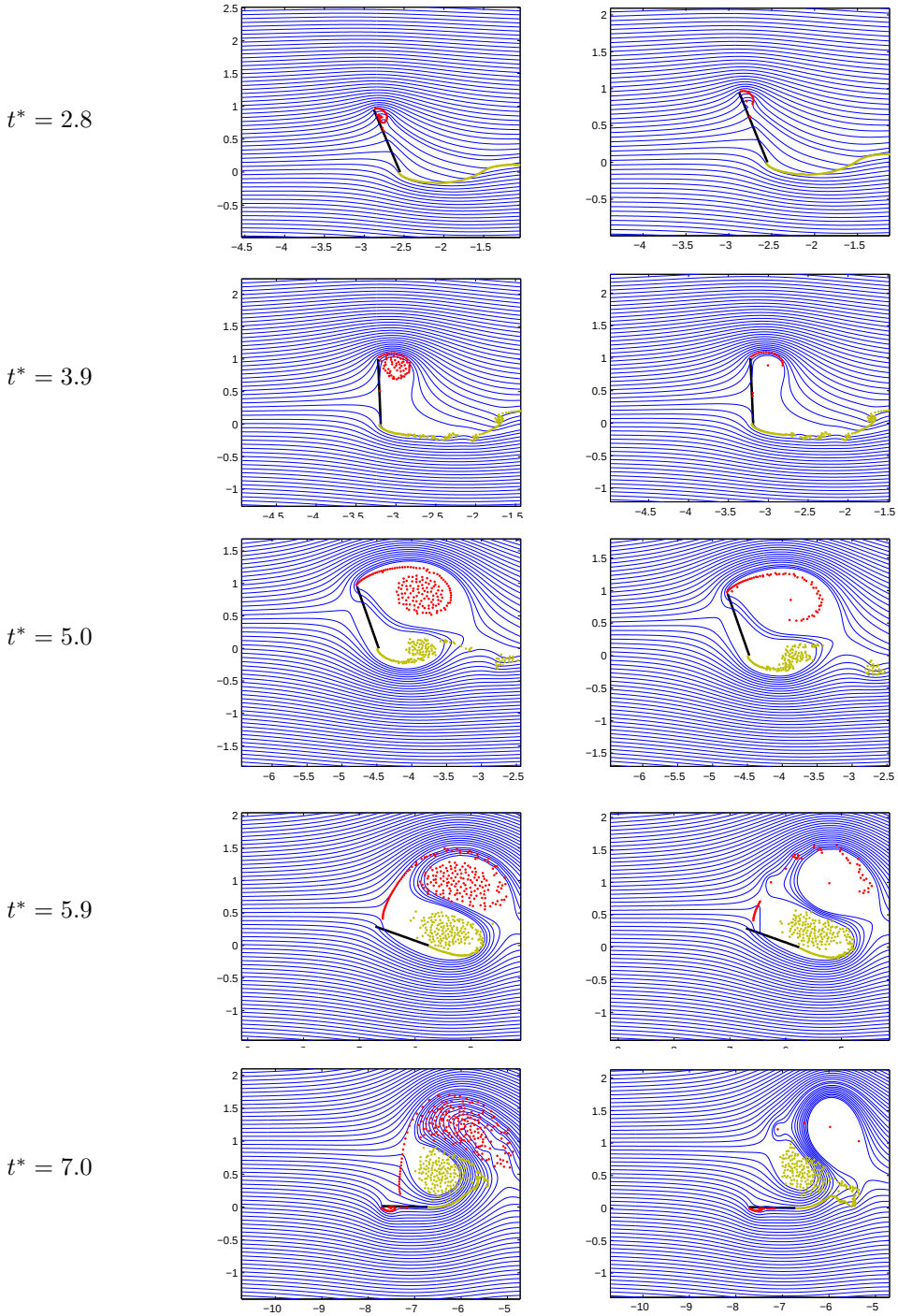

Figure 6. Case 2: Streamline patterns predicted by LDVM (left) and the reduced order method (right) at five time instants.

slight discrepancy compared to the prediction of LDVM. At the end of the motion, the reduced order model predicts the leading edge vorticity in the flow field using just 36 DVs whereas the LEV structure in LDVM is represented by 274 DVs. Computation time savings in using the reduced order model is evident in the run time of 6.9 s for the reduced order model as compared to 10.6 s for LDVM.

C. Case 3: Flat plate undergoing 0-45 pitch up-hold motion about leading edge

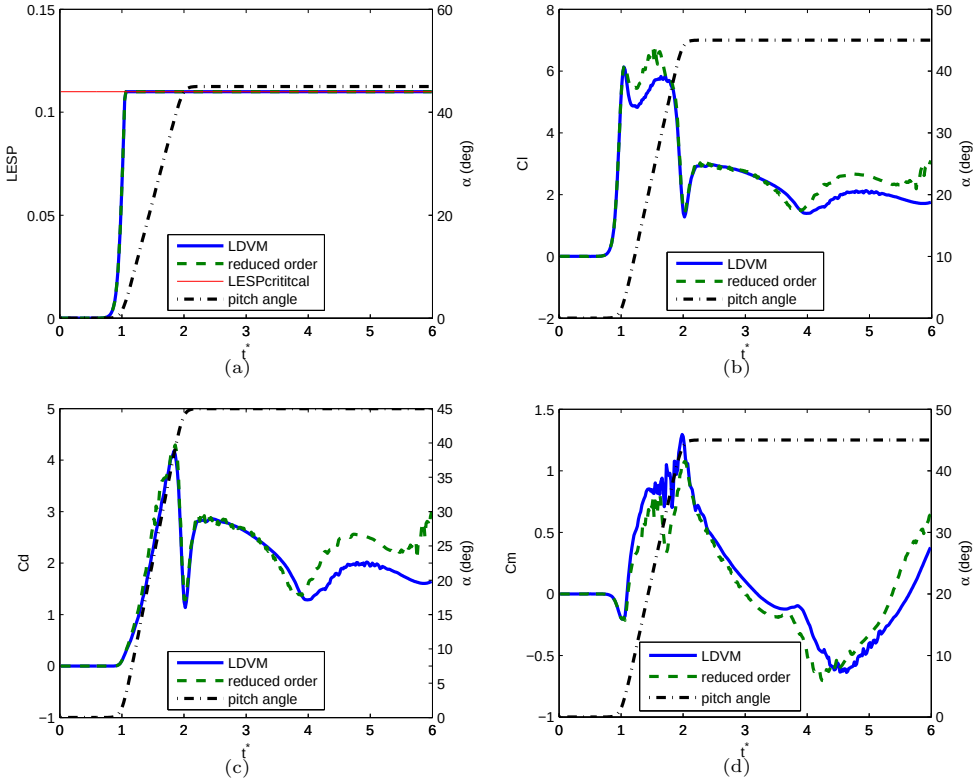

Figure 7. Case 3: Comparison of predictions of the reduced order method and LDVM. Variation with $t^* = tU/c$ of: (a) LESP, (b) lift coefficient, (c) drag coefficient, and (d) pitching moment coefficient about the quarter chord.

This case study deals with the pitch up-hold maneuver of a flat plate at a Reynolds number of 1,000. The pitch-ramp motion is generated using an Eldredge function. The flat plate pitches up about the leading edge with a non-dimensional pitch rate of $K = 0.4$. The value of critical LESP for this case is 0.11. The comparison of LESP and the time variation of force and moment coefficients between the two methods are shown in Fig. 7. Streamline patterns predicted by the two methods at different instants of time are compared in Fig. 8.

The LESP for this motion reaches the critical value when the pitch angle is approximately 3 degrees. From this instant, it stays at the critical value till the end of the motion. Consequently, vorticity is continuously shed from the leading edge from this instant till the end of the motion. The flow field predicted by LDVM is shown in Fig. 8. The shear layer starts rolling up near the leading edge, forming a cluster of discrete vortices. As time progresses, the shear layer feeds more DVs into this core, and the core grows in size. The core is seen to move away from the surface of the flat plate towards the second half of the motion. Later, the concentrated LEV structure pinches off from the shear layer. A part of the shear layer gets convected downstream with the core, while at the same time rolling up into the core. The remaining part of the shear layer that is still attached to the leading edge starts rolling up and forms another concentrated vortex structure near the LE.

It can be observed from Fig. 8 that the reduced order model replicates the initial rollup and growth of

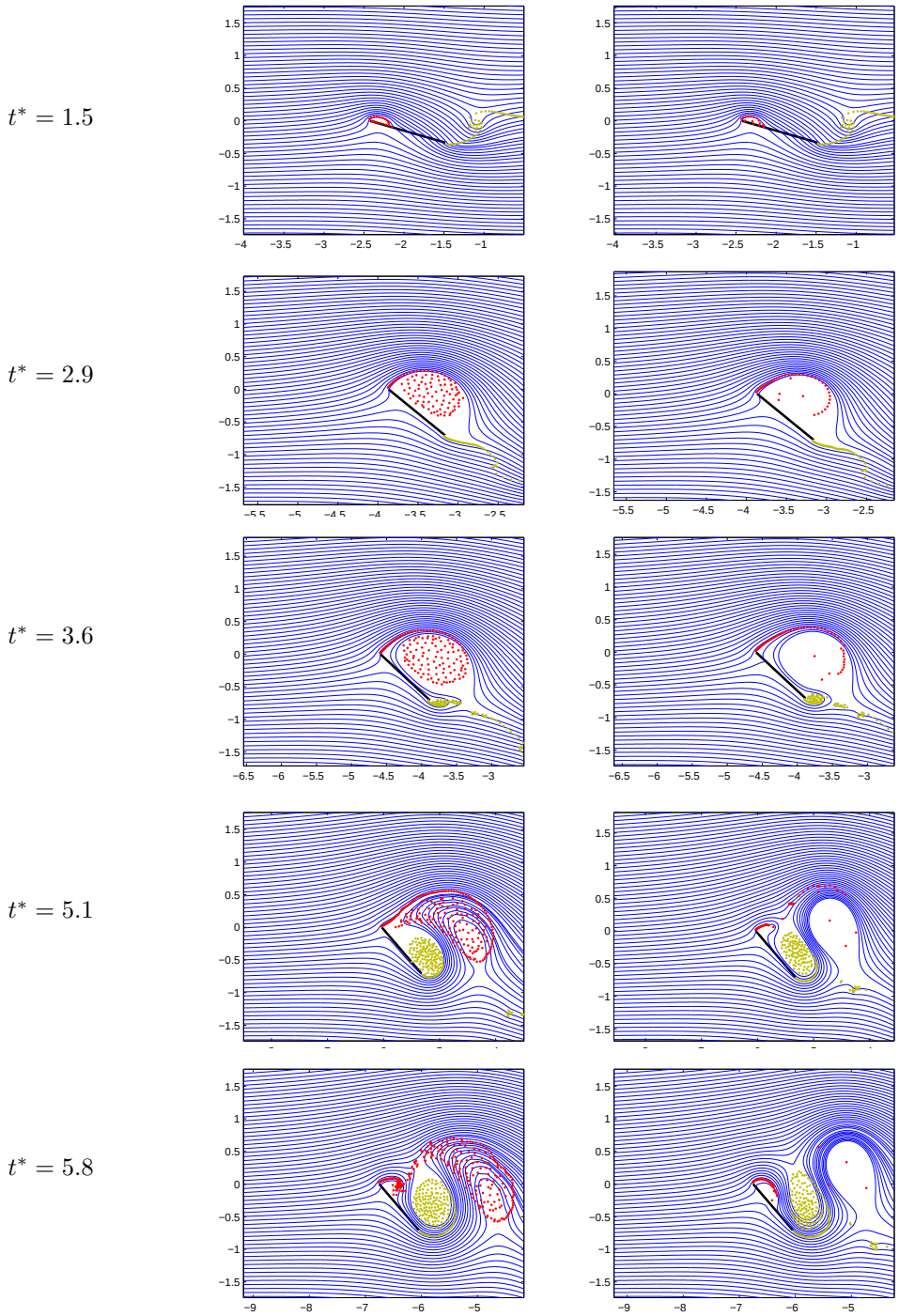

Figure 8. Case 3: Streamline patterns predicted by LDVM (left) and the reduced order method (right) at five time instants.

the LEV as well as its pinch-off. An SLEV is initiated at the instant when the initial rollup is identified. Point vortices from the shear layer are merged to this SLEV at each time step, and hence the shear layer and the concentrated vortex structure are captured by the reduced order model. The reduced order model also successfully identifies the LEV pinch-off and initiates a second SLEV to model the rollup of the tip of shear layer attached to the leading edge. Following this,the DVs in the shear layer associated with the first SLEV are merged to it at every time step. Simultaneously, the ones in the shear layer associated with the second SLEV are merged to the second SLEV. However, the reduced order model predicts pinch-off a little earlier compared to LDVM. This can be noted from the streamline plot at $t^* = 5.1$. At this time instant, a pinch-off is not yet visible according to the predictions of LDVM; but a pinch-off is seen to be taking place according to the reduced order model. A significant interaction of the trailing edge vorticity with the LEV core precedes the pinch-off in LDVM. This may need to be taken care of for eliminating the discrepancy in the predictions of the reduced order model.

It can be observed from the LESP and force and moment coefficient history plots in Fig. 7 that the reduced order model accurately predicts these quantities till there is significant interaction of leading edge vorticity with the LEV in addition to replicating the flow field. However, there are slight discrepancies after the interaction becomes strong. This is evident in the streamline plots. The trailing edge vorticity starts interacting with the LEV after $t^* = 3.6$. The lift and drag coefficient predictions of the reduced order model show mismatch approximately after this instant of time.

At the end of the motion, LDVM has 260 DVs in the simulation for modeling the leading edge vorticity whereas the reduced order model has just 38 DVs. Owing to the reduction in number of discrete vortices compared to the first two cases, a reduction in computational time has been obtained with the reduced order model for this case. The run time of the reduced order model was 13.6 seconds whereas it took 17.1 seconds for the LDVM code to generate the results.

Table 1 provides a comparison of performance of the new reduced order model with that of LDVM in terms of the discrete vortex count and run time.

Case No.	Discrete LEV count LDVM	Discrete LEV count reduced order	Run time LDVM (seconds)	Run time reduced order (seconds)
1	380	89	29.3	20.1
2	274	36	10.6	6.9
3	260	38	17.1	13.6

Table 1. Comparison of run times for the three cases between LDVM and the reduced order method

V. Conclusions and future work

In this paper, we presented an approach to reduce the vortex count in discrete vortex methods for modeling unsteady aerodynamic flows. We proposed a phenomenological approach to modeling the leading edge vortex from 2D bodies undergoing unsteady motion. We proposed an algorithm to identify the initial roll-up of the shear layer shed from the leading edge, and to reduce the discrete vortex count by merging suitable pairs of discrete vortices. The model has the capability to handle intermittent LEV shedding and LEV pinch-off. The reduced order model shows promise in terms of reducing the count of discrete vortices compared to the higher order LDVM model, and thus, saving computation time significantly, while also giving predictions of forces and moments close to that of the higher order method. The method is found to be more efficient in cases where there are large number of LEVs in the higher order method.

The predictions of the model deviate from that of the higher order method when there is significant interaction between the vorticity shed from the leading and trailing edges. The model needs to be adapted to better handle such situations. The algorithm can be implemented to reduce the discrete trailing edge vortex count, and achieve faster computation times.

Acknowledgements

The authors wish to gratefully acknowledge the support of the U.S. Air Force Office of Scientific Research through grant FA 9550-13-1-0179 and program managers Dr. Douglas Smith and Dr. Ivett Leyva.

References

[1]Ramesh, K., Gopalarathnam, A., Edwards, J. R., Ol, M. V., and Granlund, K., "An Unsteady Airfoil Theory Applied to Pitching Motions Validated Against Experiment and Computation," *Theoretical and Computational Fluid Dynamics*, Vol. 27, No. 6, 2013, pp. 843–864.

[2]Leishman, J. G., *Principles of Helicopter Aerodynamics*, Cambridge Aerospace Series, 2002.

[3]Wagner, H., "Über die Entstehung des dynamischen Auftriebes von Tragflügeln," *ZaMM*, Vol. 5, No. 1, 1925, pp. 17–35.

[4]Theodorsen, T., "General Theory of Aerodynamic Instability and the Mechanism of Flutter," NACA Rept. 496, 1935.

[5]McGowan, G. Z., Granlund, K., Ol, M. V., Gopalarathnam, A., and Edwards, J. R., "Investigations of lift-based pitch-plunge equivalence for airfoils at low Reynolds numbers," *AIAA Journal*, Vol. 49, No. 7, 2011, pp. 1511–1524.

[6]Ol, M. V., Bernal, L., Kang, C. K., and Shyy, W., "Shallow and deep dynamic stall for flapping low Reynolds number airfoils," *Experiments in Fluids*, Vol. 46, No. 5, 2009, pp. 883–901.

[7]Garmann, D. J. and Visbal, M. R., "Numerical investigation of transitional flow over a rapidly pitching plate," *Physics of Fluids*, Vol. 23, 2011, pp. 094106.

[8]Granlund, K., Ol, M. V., and Bernal, L. P., "Unsteady pitching flat plates," *Journal of Fluid Mechanics*, Vol. 733, No. 1, 2013, pp. R5(13 pages).

[9]Pitt Ford, C. W. and Babinsky, H., "Lift and the leading-edge vortex," *Journal of Fluid Mechanics*, Vol. 720, No. 1, 2013, pp. 280–313.

[10]Baik, Y. S., Bernal, L. P., Granlund, K., and Ol, M. V., "Unsteady force generation and vortex dynamics of pitching and plunging aerofoils," *Journal of Fluid Mechanics*, Vol. 709, No. 1, 10 2012, pp. 37–68.

[11]Rival, D. E., Kriegseis, J., Schaub, P., Widmann, A., and Tropea, C., "Characteristic length scales for vortex detachment on plunging profiles with varying leading-edge geometry," *Experiments in Fluids*, January 2014, DOI: 10.1007/s00348-013-1660-x.

[12]Clements, R. R. and Maull, D. J., "The representation of sheets of vorticity by discrete vortices," *Progress in Aerospace Sciences*, Vol. 16, No. 2, 1975, pp. 129–146.

[13]Saffman, P. G. and Baker, G. R., "Vortex interactions," *Annual Review of Fluid Mechanics*, Vol. 11, No. 1, 1979, pp. 95–121.

[14]Leonard, A., "Vortex methods for flow simulation," *Journal of Computational Physics*, Vol. 37, No. 3, 1980, pp. 289–335.

[15]Sarpkaya, T., "An inviscid model of two-dimensional vortex shedding for transient and asymptotically steady separated flow over an inclined plate," *Journal of Fluid Mechanics*, Vol. 68, No. 01, 1975, pp. 109–128.

[16]Clements, R. R., "An inviscid model of two-dimensional vortex shedding," *Journal of Fluid Mechanics*, Vol. 57, No. 2, 1973, pp. 321–336.

[17]Kiya, M. and Arie, M., "A contribution to an inviscid vortex-shedding model for an inclined flat plate in uniform flow," *Journal of Fluid Mechanics*, Vol. 82, No. 2, 1977, pp. 241–253.

[18]Katz, J., "Discrete vortex method for the non-steady separated flow over an airfoil," *Journal of Fluid Mechanics*, Vol. 102, No. 1, 1981, pp. 315–328.

[19]Ansari, S. A., Żbikowski, R., and Knowles, K., "Non-linear unsteady aerodynamic model for insect-like flapping wings in the hover. Part 1: methodology and analysis," *Proceedings of the Institution of Mechanical Engineers, Part G: Journal of Aerospace Engineering*, Vol. 220, No. 2, 2006, pp. 61–83.

[20]Wang, C. and Eldredge, J. D., "Low-order phenomenological modeling of leading-edge vortex formation," *Theoretical and Computational Fluid Dynamics*, Vol. 27, No. 5, 2012, pp. 577–598.

[21]Ramesh, K., Gopalarathnam, A., Granlund, K., Ol, M. V., and Edwards, J. R., "Discrete-vortex method with novel shedding criterion for unsteady airfoil flows with intermittent leading-edge vortex shedding," *Journal of Fluid Mechanics*, Vol. 751, 2014, pp. 500–538.

[22]Brown, C. E. and Michael, W. H., "Effect of leading edge separation on the lift of a delta wing," *Journal of Aerospace Sciences*, Vol. 21, 1954, pp. 690–694.

[23]Wang, C. and Eldredge, J. D., "Low-order phenomenological modeling of leading-edge vortex formation," *Theoretical Computational Fluid Dynamics*, Vol. 27, 2013, pp. 577–598.

[24]Howe, M. S., "Emendation of the Brown Michael equation, with application to sound generation by vortex motion near a half-plane," *Journal of Fluid Mechanics*, Vol. 329, 1996, pp. 89–101.

[25]Cortelezzi, L. and Leonard, A., "Point vortex model of the unsteady separated flow past a semi-infinte plate with transverse motion," *Fluid Dynamics Research*, Vol. 11, 1993, pp. 263–295.

[26]Darakananda, D., Eldredge, J. D., Colonius, T., and Williams, D. R., "A vortex sheet/point vortex dynamical model for unsteady separated flows," AIAA Paper 2016–2072, Jan. 2016.

[27]Milano, M. and Gharib, M., "Uncovering the physics of flapping plates with artificial evolution," *Journal of Fluid Mechanics*, Vol. 534, 2005, pp. 403–409.

[28]Rival, D., Prangemeier, T., and Tropea, C., "The influence of airfoil kinematics on the formation of leading-edge vortices in bio-inspired flight," *Experiments in Fluids*, Vol. 46, 2009, pp. 823–833.

[29]Rival, D., Kriegseis, J., Schaub, P., Widmann, A., and Tropea, C., "Characteristic length scales for vortex detachment on plunging profiles with varying leading-edge geometry," *Experiments in Fluids*, Vol. 55, No. 1, 2014, pp. 18.

[30]Antonini, E. G. A., Bedon, G., Betta, S. D., Michelini, L., Castelli, M. R., and Benini, E., "Innovative Discrete-Vortex Model for Dynamic Stall Simulations," *AIAA Journal*, Vol. 53, 2015, pp. 479–485.

[31]Cortelezzi, L., *A theoretical and computational study on active wake control*, Ph.D. thesis, California Institute of Technology, 1992.

[32]Sarpkaya, T., "An inviscid model of two-dimensional vortex shedding for transient and asymptotically separated flow over an inclined plate," *Journal of Fluid Mechanics*, Vol. 68, No. 1, 1975, pp. 109–128.

[33]Moore, D. W., "A numerical study of the roll-up of a finite vortex sheet," *Journal of Fluid Mechanics*, Vol. 63, No. 2, 1974, pp. 225–235.

[34]Nair, A. G. and Taira, K., "Network-theoretic approach to sparsified discrete vortex dynamics," *Journal of Fluid Mechanics*, Vol. 768, 2015, pp. 549–571.

[35]Katz, J. and Plotkin, A., *Low speed aerodynamics*, Cambridge University Press, 2000.

[36]Ramesh, K., Gopalarathnam, A., Granlund, K., Ol, M. V., and Edwards, J. R., "Discrete-vortex method with novel shedding criterion for unsteady airfoil flows with intermittent leading-edge vortex shedding," *Journal of Fluid Mechanics*, Vol. 751, 2014, pp. 500–538.

[37]Ansari, S. A., Zbikowski, R., and Knowles, K., "Nonlineary unsteady aerodynamic model for insect-like flapping wings in hover. Part 1: Methodology and analysis," *Proceedings of the Institution of Mechanical Engineers, Part G: Journal of Aerospace Engineering*, Vol. 220, No. 3, 2006, pp. 169–186.

[38]Vatistas, G. H., Kozel, V., and Mih, W. C., "A simpler model for concentrated vortices," *Experiments in Fluids*, Vol. 11, No. 1, 1991, pp. 73–76.